Measurement of Landau Damping and the Evolution to a BGK Equilibrium

J. R. Danielson, F. Anderegg, and C. F. Driscoll

Department of Physics and Institute for Pure and Applied Physical Sciences, University of California at San Diego, La Jolla, California 92093, USA

(Received 20 February 2004; published 18 June 2004)

Linear Landau damping and nonlinear wave-particle trapping oscillations are observed with standing plasma waves in a trapped pure electron plasma. For low wave amplitudes, the measured linear damping rate agrees quantitatively with linear Landau damping theory. At larger amplitudes, the wave initially damps at the Landau rate, then regrows and oscillates, approaching a steady state, as predicted by O'Neil in 1965 [Phys. Fluids **8**, 2255 (1965)]. This BGK equilibrium is observed to decay slowly due to external dissipation.

DOI: 10.1103/PhysRevLett.92.245003 PACS numbers: 52.27.Jt, 52.20.–j, 52.35.Fp, 52.35.Sb

The first experiments to demonstrate linear Landau damping measured the spatial damping length of Trivelpiece-Gould (TG) waves in an open-ended neutral plasma column [1]. TG waves are longitudinal electrostatic plasma oscillations (Langmuir waves), modified by the cylindrical boundary [2]. Landau damping occurs when resonant electrons moving at the wave phase velocity, v_ϕ, absorb energy from the wave [3]. At large wave amplitudes, nonlinear trapping oscillations were also observed in these plasmas [4] and shown to occur when the resonant electrons become trapped in the wave potential, as predicted by O'Neil [5]. Other nonlinear effects such as plasma wave echoes [6] and sideband frequency generation [7] were also observed.

The time-asymptotic state of a large amplitude Landau damped wave is predicted to be a "BGK" (Bernstein-Greene-Kruskal) equilibrium [5,8]. However, previous experimental attempts to observe BGK states have been inhibited by the robust sideband instability [9]. Recently, several authors have argued theoretically that the wave amplitude continues to decay to zero and never forms a BGK mode [10,11]. In response, other authors have supported the existence of BGK steady states through asymptotic theory [12,13] and long-time plasma simulations [14].

In this Letter, we report the first observation of Landau damping in the linear regime, in a trapped plasma. Here, the same particles interact with the wave for a long time ($\sim$1000 wave periods) and have the possibility of forming a BGK state. This situation is similar to previous observations of "bounce-resonant" Landau damping in a neutral plasma confined in a mirror machine [15,16]. However, in the current experiments the excited modes are discrete oscillations of the plasma column [17] which are only weakly damped and which cannot resonantly couple to sideband oscillations. Further, we measure the late time evolution of large amplitude waves, where particle trapping dominates and Landau damping is substantially diminished. The measured wave amplitude oscillation frequencies are in good agreement with theory, and the waves are observed to evolve to a BGK equilibrium. At late times, this state is observed to decay slowly due to finite dissipation from our detection equipment. In contrast to the recently reported "bucket-BGK" modes which have no linear wave limit [18], we observe the temporal evolution of a Landau damped wave to a BGK equilibrium. Our experimental results validate the physical picture used in recent numerical simulations [14].

The waves are excited in pure electron plasma columns contained in two similar Penning-Malmberg traps (*EV* and *IV*). These two traps differ mainly in plasma diameter and magnetic field strength. The *EV* trap consists of a series of hollow conducting cylinders of radius $r_w = 3.8$ cm contained in ultrahigh vacuum at $P \approx 10^{-10}$ Torr with a uniform magnetic field of $B \leq 0.375$ kG. Typical plasmas have $N_{\rm tot} \approx 10^9$ electrons in a column length $L_p \approx 24$ cm with a plasma radius $r_p \approx 1.0$ cm and a central density $n_0 \approx 10^7$ cm^{-3}. (For *IV*, the parameters are $B = 30$ kG, $r_p \approx 0.2$ cm, $r_w = 2.86$ cm, and $L_p \simeq 41$ cm.)

The plasma density profile $n(r)$ and temperature T_p are obtained by dumping the plasma axially and measuring the total charge passing through a hole in a scanning collimator plate. Both measurements require shot-to-shot reproducibility of the injected plasma, and we typically observe variability $\delta Q/Q \leq 1\%$. On *IV*, a weak "rotating wall" (RW) drive at $f_{\rm RW} \sim 0.5$ MHz is used to obtain steady-state confinement of the electron column [19]. The *EV* plasmas expand radially towards the wall with a characteristic time of $\tau_m \approx 100$ sec, whereas the wave experiments presented here require only a time $t < 0.5$ sec.

The parallel temperature $T_\parallel$ of the electrons is measured by slowly lowering the confinement voltage and measuring the escaping charge [20]. On *EV*, the perpendicular temperature $T_\perp$ is also measured using a "magnetic beach" analyzer. In general, we find $T_\parallel \approx T_\perp \equiv T_p$, since the electron-electron collision rate $\nu_{\perp\parallel} \approx 100$ sec^{-1} is relatively rapid [21]. On *EV*, the electrons equilibrate to $T_p \approx 1$ eV soon after injection, whereas the electrons in *IV* cool to $T_p \approx 0.05$ eV due to cyclotron radiation. To control the temperature, we apply auxiliary "wiggle" heating by modulating one electrode voltage at a frequency $f_h = 0.8$–1.0 MHz, where f_h is adjusted so that all harmonics are distinct from the TG mode of interest [22].

We excite plasma waves by applying sinusoidal voltages of amplitude $V_{\rm exc}$ and frequency ω to a cylindrical electrode at one end of the column. The wave density perturbation δn induces a measured antenna voltage V_a on a separate receiving electrode. The experiments are performed in two complementary ways: a continuous transmission with slowly swept frequency, and a resonant burst excitation with temporal response detected with a wide bandwidth receiver. In the swept spectrum measurement the damping rate is obtained from the half-width of the (approximately Lorentzian) resonance curve. For burst excitation, the damping rate is obtained directly from the exponential decay of the received signal. The two techniques give essentially identical linear damping rates.

We study the damping of azimuthally symmetric ($m_\theta = 0$) standing TG modes in the range of $\omega/2\pi \simeq$ 1–10 MHz. For the case of thin plasmas ($r_p \ll r_w$), the dispersion relation can be approximated by

$$\omega_{\rm TG} \approx \omega_p (k_z/k_\perp)[1 + (3/2)(\bar{\rm v}/{\rm v}_\phi)^2]. \tag{1}$$

Here the axial wave number is given by $k_z = \pi m_z/L_p$, with the integer axial mode number $m_z = 1, 2, \ldots, 5$, and the perpendicular wave number is set by the geometry to be $k_\perp \approx r_p^{-1}[2/\ln(r_w/r_p)]^{1/2}$. The wave frequency scales with the plasma frequency $\omega_p/2\pi =$ 28 MHz $(n/10^7\ {\rm cm}^{-3})^{1/2}$, reduced by the ratio of the perpendicular wavelength to axial wavelength [23]. We have also included the lowest order thermal correction which depends on the ratio of thermal velocity to wave phase velocity, $\bar{\rm v}/{\rm v}_\phi = (T_p/m)^{1/2}/(\omega/k_z)$. In contrast to previous experiments [1], the measurements to be presented were taken in the "acoustic" ($\omega \propto k_z$) part of the dispersion relation where the wave phase velocity is nearly independent of the mode frequency.

The dispersion relation also gives a relationship between the perturbed density (δn) and the measured image charge on the receiving antenna (Q_a). Since the attached amplifier, with input impedance $Z_{\rm ext}$, converts the induced image current to a voltage ($V_a = I_a Z_{\rm ext} = \omega Q_a Z_{\rm ext}$), the measured antenna voltage at the wall is related to the wave density perturbation by

$$\frac{\delta n}{n_0} \approx \left(\frac{\pi m_z}{\hat{f} J_0(r_p k_\perp)}\right) \frac{V_a/\omega Z_{\rm ext}}{e N_{\rm tot}}, \tag{2}$$

where J_0 is a Bessel function, z_1 and z_2 are the left and right ends of the receiver electrode, and $\hat{f} = \sin(k_z z_2) - \sin(k_z z_1)$ accounts for the finite overlap of the receiving electrode with the plasma wave. Similarly, we calculate the axial electric field to be

$$\delta E_z \approx \left(\frac{2}{\hat{f}} \frac{\ln(r_w/r_p)}{J_0(r_p k_\perp)}\right) k_z^2 \frac{V_a}{\omega Z_{\rm ext}}. \tag{3}$$

These modes are predicted to damp exponentially at a rate $\gamma_{\rm total}$, which is the sum of $\gamma_{\rm LD}$ from internal Landau damping (LD), and $\gamma_{\rm ext}$ due to dissipative loading by the external receiver, i.e., $\gamma_{\rm total} = \gamma_{\rm LD} + \gamma_{\rm ext}$. To lowest order (assuming ${\rm v}_\phi \gg \bar{\rm v}$), linear Landau damping for a Maxwellian velocity distribution is given by [3]

$$\frac{\gamma_{\rm LD}}{\omega} \simeq \sqrt{\frac{\pi}{8}} \left(\frac{{\rm v}_\phi}{\bar{\rm v}}\right)^3 \exp\left\{-\frac{1}{2}\left(\frac{{\rm v}_\phi}{\bar{\rm v}}\right)^2\right\}. \tag{4}$$

Nonlinear trapping will reduce this damping rate for large amplitude waves. However, the mode damping $\gamma_{\rm ext}$ from the detection amplifier is independent of wave amplitude and typically in the range of $10^{-4} \lesssim \gamma_{\rm ext}/\omega \lesssim 10^{-3}$, depending on the mode frequency and details of the measurement circuit. For very large amplitude waves, with Landau damping strongly reduced by particle trapping, the minimum measured damping rate will be set by $\gamma_{\rm ext}$.

Temporal evolutions of burst-excited modes with $\omega/2\pi = 3.5$ MHz are shown in Fig. 1, for ten cycle bursts of amplitude $V_{\rm exc} = 4$–30 mV. At the lowest amplitude, the mode is seen to decay exponentially with a measured linear damping rate $\gamma_L/\omega = 5 \times 10^{-3}$. As $V_{\rm exc}$ is increased, the overall mode decay rate is diminished and oscillations in the mode amplitude develop, with an oscillation frequency that increases as $V_{\rm exc}$ increases. At the largest amplitudes, there is little amplitude decay during the first several oscillations, and only a very weak decay ($\gamma_{\rm ext}/\omega \sim 10^{-4}$) afterwords.

This transition from fast decay at low amplitudes to weak decay at large amplitudes is also observed in continuous transmission resonance experiments. In Fig. 2, we plot the received peak amplitude (on resonance) and the mode damping (resonance width) over a broad range of amplitudes. We observe three distinct regimes: (i) a small amplitude, fast damping rate regime, independent of excitation amplitude down to thermally excited levels [24]; (ii) a nonlinear damping regime, where the damping rate decreases with increasing excitation amplitude, and

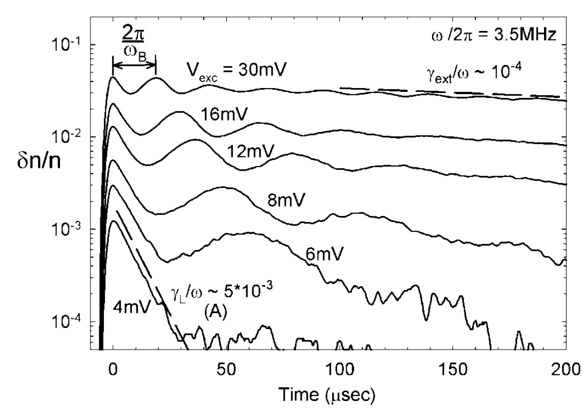

FIG. 1. Detected amplitude versus time after ten cycle bursts for different $V_{\rm exc}$. Note the factor of 50 drop in the wave damping rate due to particle trapping.

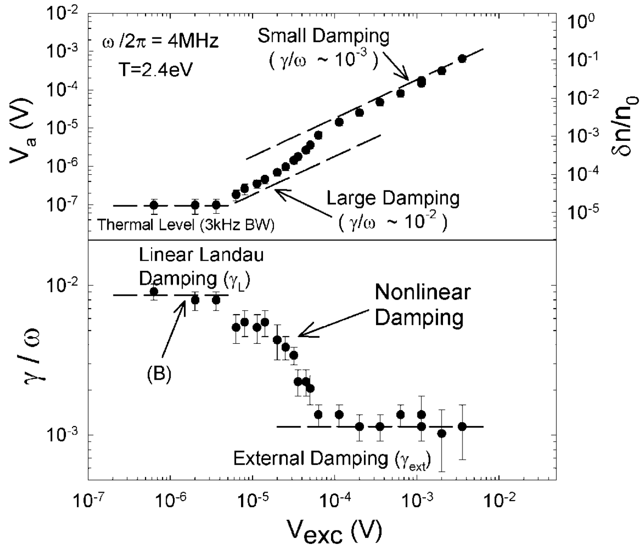

FIG. 2. Amplitude at resonance and damping rate versus excitation amplitude during a transmission experiment.

giving a corresponding increase in the received peak amplitude at fixed excitation, and (iii) a large amplitude, weak damping regime, where the damping rate is again independent of excitation amplitude and is determined by the dissipation in the detection circuit.

Figure 3 shows the measured small amplitude damping rate γ_L/ω versus temperature, characterized by $\bar{\mathrm{v}}^2/\mathrm{v}_\phi^2$. The sharp exponential increase in the damping rate for $3 < \mathrm{v}_\phi/\bar{\mathrm{v}} < 5$ is in quantitative agreement with the predictions of linear Landau damping (solid curve). The open squares are from the *IV* apparatus, and the gray squares and black triangles are from the *EV* apparatus. Even though the plasma parameters are substantially different, with correspondingly different wave phase velocities, all of the data are consistent with linear Landau damping plus a fixed external damping.

Where Landau damping is dominant, the primary source of uncertainty is in estimating the wave phase velocity $\mathrm{v}_\phi = \omega/k_z \approx \omega L_p/\pi m_z$. Here L_p is found from the z-integrated charge and a self-consistent Poisson-Boltzman solution, constrained by the known boundary conditions. However, the finite length of the plasma tends to increase the effective mode wavelength, and hence the wave velocity, by an amount that scales like R_p/L_p [17]. For the *IV* data in Fig. 3, this effect is negligible, whereas for the *EV* data, this effect can be as high as 10%. Further, at low temperatures, the lowest measured damping rate ($\gamma_{\mathrm{ext}}/\omega \sim 5 \times 10^{-4}$) is consistent with dissipation from $R \sim 50\ \Omega$ in parallel with $C \sim 200$ pF on the external electronics.

To further investigate the nonlinear regime, we return to Fig. 1 and define two quantities for comparison to theory. First, the initial damping of the wave, as before, is defined to be γ_L. This rate is identical to the spectrum measurements in the low amplitude regime and is shown by the "triangles" in Fig. 3. This fast initial damping corresponds to linear Landau damping. Second, we define an amplitude bounce frequency ω_B by measuring the time Δt between the peak of the excitation and the peak of the first oscillation, with $\omega_B \equiv 2\pi/\Delta t$.

In essence, large amplitude waves trap the resonant electron population before the wave has time to damp. These resonant electrons become trapped in the wave potential well during a time $1/\omega_T \equiv \sqrt{m/e\delta E_z k_z}$ [5]. As the electrons bounce back and forth inside of the potential well of the wave, the amplitude of the wave periodically grows and damps. Eventually the motion of the trapped electrons will phase mix, causing the amplitude of the wave to become constant with time. This is the classic development of what is referred to as a BGK equilibrium [5,8], a stable plasma equilibrium with an undamped nonlinear plasma wave.

The measured amplitude oscillation frequencies ω_B for different excitation amplitudes are compared to theory in Fig. 4. Here, the initial amplitude of the excited wave is used to calculate the axial electric field of the wave δE_z from Eq. (3), giving the initial electron trapping frequency ω_T. The dashed line is the O'Neil theory, which is valid only in the limit of large (and constant) electric field ($\omega_T/\gamma_{\mathrm{L}} \gg 1$) [5]. The solid line is a numerical calculation accounting for the instantaneous wave electric field, similar to the calculation done in Ref. [25].

The predictions for ω_B/γ_L depend only on the ratio of the initial trapping frequency to the linear Landau damping rate, so the data are plotted versus ω_T/γ_L. Data are shown for experiments at two different temperatures, and correspondingly two different linear damping rates. The

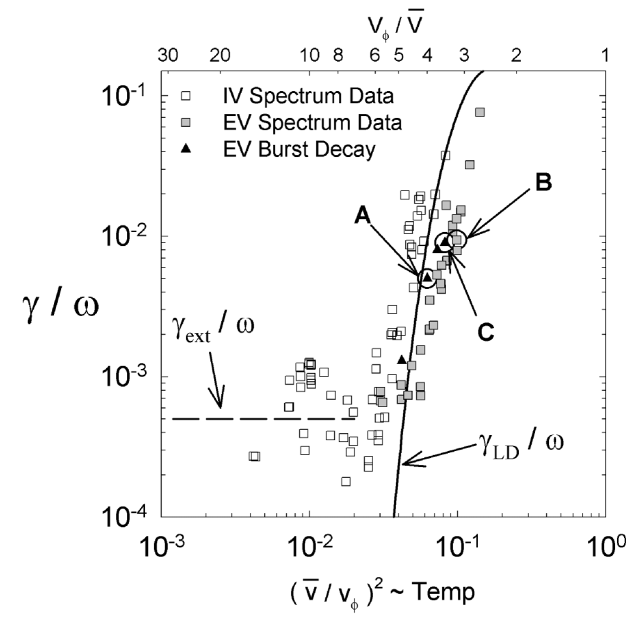

FIG. 3. Internal (linear) damping rate versus temperature, with temperature normalized as $\bar{\mathrm{v}}^2/\mathrm{v}_\phi^2$ in order to compare all experiments to a single theory curve. The solid line is the linear Landau damping prediction from Eq. (4). The letters A, B, and C designate data points from Figs. 1, 2, and 4.

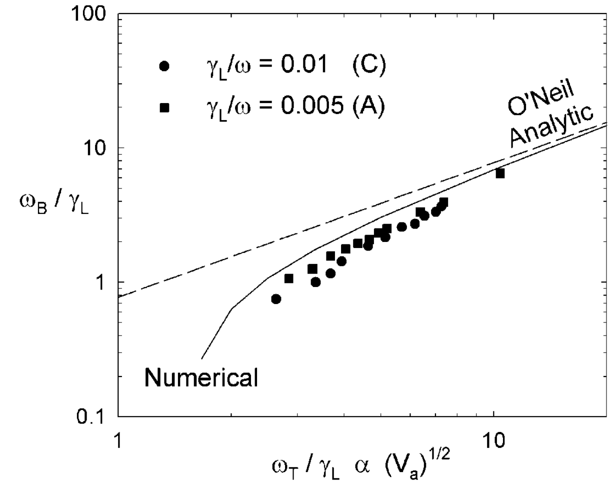

FIG. 4. Measured nonlinear amplitude "bounce" frequency ω_B versus calculated trapping frequency ω_T for two different levels of Landau damping.

scaling agreement between the measurements and theory indicates that trapping oscillation theory applies to standing waves in a trapped non-neutral plasma. The measurements of ω_B are 10%–40% lower than predicted. This could be caused by several effects, including detrapping of resonant electrons [26] and collisional repopulation [27]; both would decrease the rate of wave regrowth and slow the amplitude bounce. Further, the effect of the external dissipation is estimated to be less than 10% and not the main cause of the deviations.

Historically, large amplitude Landau damped waves in neutral plasma columns have typically been unstable to sideband generation, which takes energy from the wave, and destroys the equilibrium [9]. Finite length non-neutral plasma columns have only a discrete spectrum of TG modes; thus no sideband instability is present, and the possibility exists for the observation of a BGK equilibrium. For the largest amplitude wave evolution of Fig. 1, the asymptotic $\gamma/\omega \sim 10^{-4}$ demonstrates that after 300 wave cycles, three nonlinear bounce periods, and about five linear Landau damping times, the BGK mode amplitude changes by only 5%. Of course, electron-electron collisions are predicted to repopulate the resonant particles, allowing the damping to resume on some time scale [27]. An amplifier with a lower impedance, and hence less external damping, would be required for a quantitative comparison with collision-induced asymptotic damping.

In conclusion, we have measured temporal Landau damping in a trapped, finite length, non-neutral plasma. We find good agreement between the measured linear damping rate and Landau damping. We also find good agreement between the measured transition to nonlinear trapping oscillations at large amplitudes with a numerical calculation that uses the evolution of the electric field self-consistently. Further, the late time evolution of these Landau damped waves is observed to approach a steady-state amplitude which is consistent with a BGK equilibrium.

This work was supported by ONR Grant No. N00014-96-1-0239 and by NSF Grant No. PHY-9876999. We thank N. Shiga for significant contributions to the data in Fig. 3, and we also thank R.W. Gould and T. M. O'Neil for many useful discussions.

[1] J. H. Malmberg and C. B. Wharton, Phys. Rev. Lett. **13**, 184 (1964).
[2] A.W. Trivelpiece and R.W. Gould, J. Appl. Phys. **30**, 1784 (1959).
[3] L. D. Landau, J. Phys. (Moscow) **10**, 45 (1946).
[4] J. H. Malmberg and C. B. Wharton, Phys. Rev. Lett. **19**, 775 (1967); R. N. Franklin, S. M. Hamberger, and G. J. Smith, Phys. Rev. Lett. **29**, 914 (1972).
[5] T. M. O'Neil, Phys. Fluids **8**, 2255 (1965).
[6] J. H. Malmberg, C. B. Wharton, R.W. Gould, and T. M. O'Neil, Phys. Rev. Lett. **20**, 95 (1968).
[7] C. B. Wharton and J. H. Malmberg, Phys. Fluids **11**, 1761 (1968).
[8] I. B. Bernstein, J. M. Green, and M. D. Kruskal, Phys. Rev. **108**, 546 (1957).
[9] R. N.Franklin *et al.*, Phys. Rev. Lett. **28**, 1114 (1972).
[10] G. Brodin, Phys. Rev. Lett. **78**, 1263 (1997).
[11] M. B. Isichenko, Phys. Rev. Lett. **78**, 2369 (1997).
[12] M.V. Medvedev, P. H. Diamond, M. N. Rosenbluth, and V. I. Shevchenko, Phys. Rev. Lett. **81**, 5824 (1998).
[13] C. Lancellotti and J. J. Dorning, Phys. Rev. E **68**, 026406 (2003).
[14] G. Manfredi, Phys. Rev. Lett. **79**, 2815 (1997).
[15] M. Koepke, R. F. Ellis, R. P. Majeski, and M. J. McCarrick, Phys. Rev. Lett. **56**, 1256 (1986).
[16] W. M. Sharp, H. L. Berk, and C. E. Nielsen, Phys. Fluids **22**, 1975 (1979).
[17] J. K. Jennings, R. L. Spencer, and K. C. Hansen, Phys. Plasmas **2**, 2630 (1995); S. N. Rasband and R. L. Spencer, Phys. Plasmas **10**, 948 (2003).
[18] W. Bertsche, J. Fajans, and L. Friedland, Phys. Rev. Lett. **91**, 265003 (2003).
[19] E. M. Hollmann, F. Anderegg, and C. F. Driscoll, Phys. Plasmas **7**, 2776 (2000).
[20] D. L. Eggleston *et al.*, Phys. Fluids B **4**, 3432 (1992).
[21] B. R. Beck, J. Fajans, and J. H. Malmberg, Phys. Rev. Lett. **68**, 317 (1992).
[22] B. P. Cluggish, J. R. Danielson, and C. F. Driscoll, Phys. Rev. Lett. **81**, 353 (1998).
[23] R.C. Davidson, *Physics of Non-neutral Plasmas* (Addison-Wesley, Reading, MA, 1990), Sec. 5.5.2.
[24] F. Anderegg *et al.*, Phys. Rev. Lett. **90**, 115001 (2003).
[25] I. H. Oei and D. G. Swanson, Phys. Fluids **15**, 2218 (1972).
[26] G. Pocobelli, Phys. Rev. Lett. **43**, 1865 (1979).
[27] V. E. Zakharov and V. I. Karpman, Sov. Phys. JETP **16**, 351 (1963).